

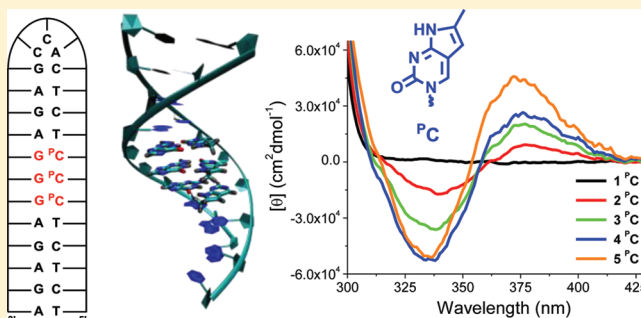
Electronic Interactions in Helical Stacked Arrays of the Modified DNA Base Pyrrolocytosine

Prakash P. Neelakandan, Martin McCullagh, George C. Schatz, and Frederick D. Lewis*

Department of Chemistry, Northwestern University, 2145 Sheridan Road, Evanston, Illinois 60208, United States

Supporting Information

ABSTRACT: The thermal stability and ultraviolet and circular dichroism spectra of nine synthetic DNA hairpins possessing one or more ^PC-G base pairs (^PC = pyrrolocytosine) have been investigated. One group of hairpins possess 1–5 sequential ^PC-G base pairs while another group possess two ^PC-G base pairs separated by 1–3 A-T base pairs. The first group displays a nearly linear dependence of UV and exciton-coupled circular dichroism (EC-CD) band intensity upon the number of neighboring chromophores, whereas the second group shows weak EC-CD only at the shortest distances between non-neighboring chromophores. This result stands in marked contrast to the exciton coupling seen between stilbene chromophores separated by as many as a dozen base pairs. The weak exciton coupling between non-neighboring ^PC chromophores, like that of the natural nucleobases, is attributed to their relatively weak electronic transition dipoles.



INTRODUCTION

Electronic interactions between the π -stacked base pairs which constitute the core of B-DNA are responsible for both the appearance of the electronic spectra of DNA and its excited state behavior.^{1,2} The latter include the formation of mutagenic TT dimers³ and the rapid decay pathways that protect cellular DNA from extensive damage caused by UV radiation.⁴ Substantial experimental and theoretical efforts have been made to understand these processes. However, there is still debate concerning the extent of electronic delocalization in both the ground and excited electronic states. Theoretical models suggest that both short-range (nearest-neighbor) and long-range interactions should contribute to the appearance of electronic spectra (absorption and circular dichroism) of helical arrays of chiral molecules.⁵ Circular dichroism provides a particularly sensitive probe of long-range electronic “communication” between chromophores.^{6,7} We have observed exciton-coupled CD spectra for pairs of stilbene and perylenediimide chromophores separated by a dozen base pairs using DNA as a helical scaffold.^{8,9} However, evidence for non-nearest-neighbor electronic interactions between natural DNA bases remains inconclusive.

DNA duplexes have weak absorption tails in their UV spectra above 300 nm; however, the relative contributions of nearest-neighbor and non-nearest-neighbor interactions to these tails are unknown.¹⁰ A recent CD investigation of single-strand oligomers having one to 30 adenines found that 190 nm excitation is delocalized over eight bases but that delocalization of the two lower energy electronic transitions was limited to nearest neighbors.¹¹ It has not been possible to study electronic delocalization in the corresponding oligomeric duplexes due to

both the instability of very short duplexes and the overlapping absorption bands of the bases in the complementary strands. The analysis of duplex electronic spectra is further complicated by the near degeneracy of the lowest excited states of the bases and the presence of multiple excited states for some of the bases.¹²

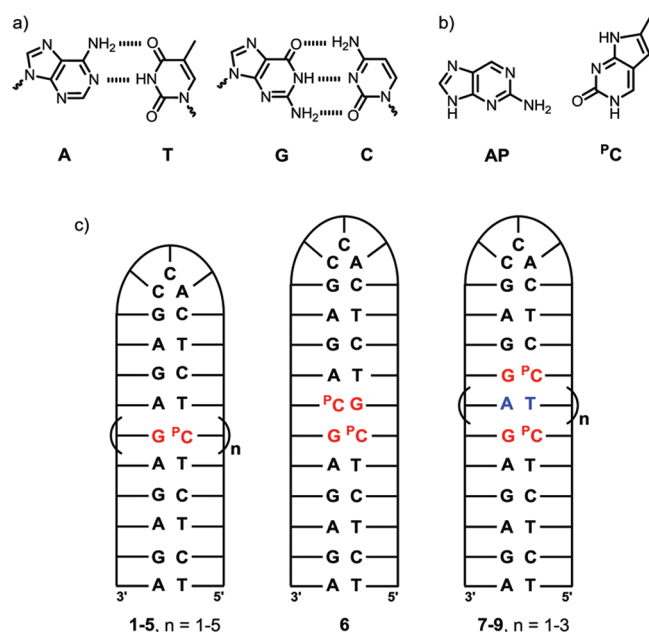
A possible solution to the problem of the overlapping absorption bands of the natural bases is provided by the use of modified nucleosides that form stable base pairs and have absorption bands at wavelengths longer than 300 nm.¹³ A number of such analogues have been developed for use in diverse applications, including the investigation of duplex formation, imaging of cellular DNA, and the study of electron transfer process in DNA.^{14,15} DNA and RNA duplex formation has also been widely exploited for the assembly of aromatic chromophores.¹⁶ Clusters of chromophores attached to nucleotides have been shown to form helical arrays on the exterior of a base-paired scaffold.^{17,18} Chromophore clusters possessing 2–6 aromatic chromophores have also been assembled within the duplex by base pair surrogates which replace both bases in the complementary strands of the duplex.^{19,20}

The use of small base analogues such as 2-aminopurine (AP)²¹ and pyrrolocytosine (^PC, Chart 1a,b)^{22–24} which mimic the ability of the natural bases to form stable base pairs provides a promising approach to the assembly of helical chromophore arrays and hence to the study of their electronic spectra. Weak excimer fluorescence has been reported for duplexes containing

Received: March 12, 2012

Published: April 9, 2012

Chart 1



multiple Ap-Ap steps,²⁵ and exciton-coupled long wavelength CD bands have been observed for duplexes possessing Ap-Ap and PC-PC steps, indicating that these chromophores adopt the right-handed helical geometry characteristic of B-DNA.^{26,27} However, attempts to prepare extended arrays of these chromophores have not been reported, and exciton coupling between separated chromophores has not been investigated.

We report here the results of an investigation of the synthesis, structure, and electronic absorption and circular dichroism spectra of the synthetic DNA hairpins 1–9 (Chart 1c) which possess one or more PC-G base pairs. Hairpins 1–5 possess 1–5 sequential PC bases within the same strand, whereas hairpin 6 has two sequential PC bases in opposite strands and 7–9 have two PC bases within the same strand separated by 1–3 T-A base pairs. Hairpins 1–9 have been characterized by their melting temperatures, UV and CD spectra, and molecular dynamics simulations, all of which are consistent with the formation of stable B-DNA structures. Much stronger exciton coupling is observed between neighboring chromophores than between chromophores located in opposite strands or separated by one or more base pairs. The absence of strong coupling between non-neighboring chromophores is attributed to the relatively weak long-wavelength electronic transition of PC, which is like those of the natural bases.

RESULTS AND DISCUSSION

Synthesis and Characterization. Oligonucleotide conjugates 1–9 (Chart 1) incorporating commercially available PC and their analogues 1'–3' (Chart S1, Supporting Information) which possess C in place of PC were prepared using standard phosphoramidite chemistry, purified using reversed-phase HPLC, and characterized by their MALDI-TOF mass (Table S1, Supporting Information), UV, and CD spectra (Table 1). The trinucleotide CCA functions as the hairpin loop for stable hairpin structures in which PC is located opposite a G and is expected to form a stable base pair.²⁸ Melting temperatures obtained from the first derivative thermal dissociation profiles measured at 260 nm (Figure S1) are reported in Table 1. The

Table 1. Spectroscopic Data for the Pyrrolocytosine Nucleobase PC and Hairpins 1–9 in 10 mM Phosphate Buffer (pH 7.2) Containing 100 mM NaCl

	T_m (ΔT_m), °C ^a	UV-vis	λ_{\max} (nm)	
			CD	
			(+), (–) ^b	(+), (–) ^c
PC		333, 258, 226		
1	74.5 (1.0)	353, 257, 209	–, 371	
2	77.5 (3.0)	350, 258, 208	379, 339	240, 229
3	86.5 (7.1)	348, 257, 208	376, 337	237, 223
4	87.5 ^d	347, 257, 209	374, 335	237, 219
5	>95 ^d	346, 258, 209	373, 334	236, 219
6	79.5	352, 258, 209		
7	79.4	353, 258, 208		
8	76.0	352, 257, 208	–, 374	
9	77.4	353, 258, 208	–, 368	

^aObtained from the first derivative thermal dissociation profiles measured at 260 nm. ^bCorresponding to the lowest energy transition of PC chromophore. ^cCorresponding to the higher energy transition of PC chromophore. ^dExtensive premelting observed (see Figure S1, Supporting Information).

thermal dissociation profiles for 4 and 5 display substantial premelting plausibly reflecting end-fraying of the hairpin tail prior to the PC-G tract and hairpin loop. Values of T_m for these hairpins are not considered to be as reliable as those of the other hairpins.

The values of T_m for 1–3 which possess 1–3 neighboring PC bases are higher than those for 1'–3' (Table S1) by 1.0, 3.0, and 7.1 °C, respectively (Table 1). Johnson et al. reported increases in T_m of 1 °C for a duplex possessing an isolated PC base and 2 °C for a duplex possessing two adjacent PC bases;²⁷ however, the large increase in T_m for 3 is without precedent. The increase in T_m for 6 and 7 is somewhat larger than that for 2. The increase in thermal stability for hairpins possessing PC-G base pairs in place of C-G base pairs is consistent with a recent theoretical investigation of the PC-G base pair²³ and is reminiscent of the increased stability of 5-methyl-C-G base pairs, which is attributed to the location of the hydrophobic methyl group within the major groove of the duplex.²⁹ Addition of chromophore arrays to the interior or exterior of a base-paired DNA scaffold typically leads to either an increase in duplex stability resulting from increased hydrophobic association^{14,30} or a decrease in duplex stability resulting from disruption of base pairing.^{17,19}

Molecular dynamics simulations were carried out for (dC₁₀) (dG₁₀) duplexes in which one, two, or three central cytosines are replaced by PC. The averaged geometry obtained for the duplex possessing three consecutive PC bases is shown in Figure 1. Top and side views show that PC-G base pairs do not disrupt the normal B-DNA π -stacking, base stacking, or base pairing in this duplex (Figure 1). The distribution of twist angles between the PC bases as well as between PC and unmodified flanking cytosine bases are peaked at 30–35° (Figure S2). These values are similar to those seen for the cytosine bases on either side of the PC stack as well as the standard twist value (36°) of base-pairs from canonical B-DNA. Similar averaged structures were obtained for duplexes possessing one or two PC bases (data not shown). While it would be desirable to obtain more direct evidence for the structures of our hairpins, X-ray and solution NMR methods

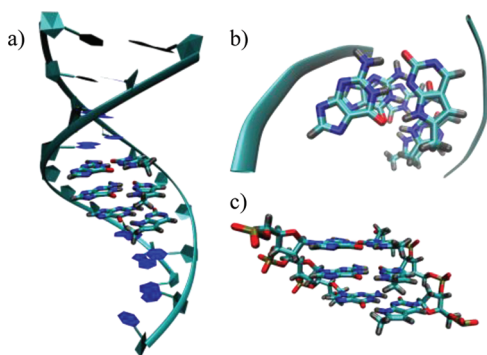


Figure 1. (a) Average geometry from a 6 ns MD simulation of the sequence (dC₁₀)(dG₁₀) wherein cytosines C₄, C₅, and C₆ are replaced with ^PC chromophores (C₁ being the 5' terminal cytosine). (b) Top and (c) side views of the three ^PC bases and paired guanines with ^PC on the right.

are time-consuming and have not been successfully applied to hairpins or duplexes containing consecutive base analogues.³¹

Ultraviolet Spectra. The UV spectra of the nucleobase ^PC and the conjugates 1–5 (normalized at 260 nm) are shown in Figure 2a with the long-wavelength spectral region (300–450 nm) shown in the inset. The long-wavelength bands of 6–9 are

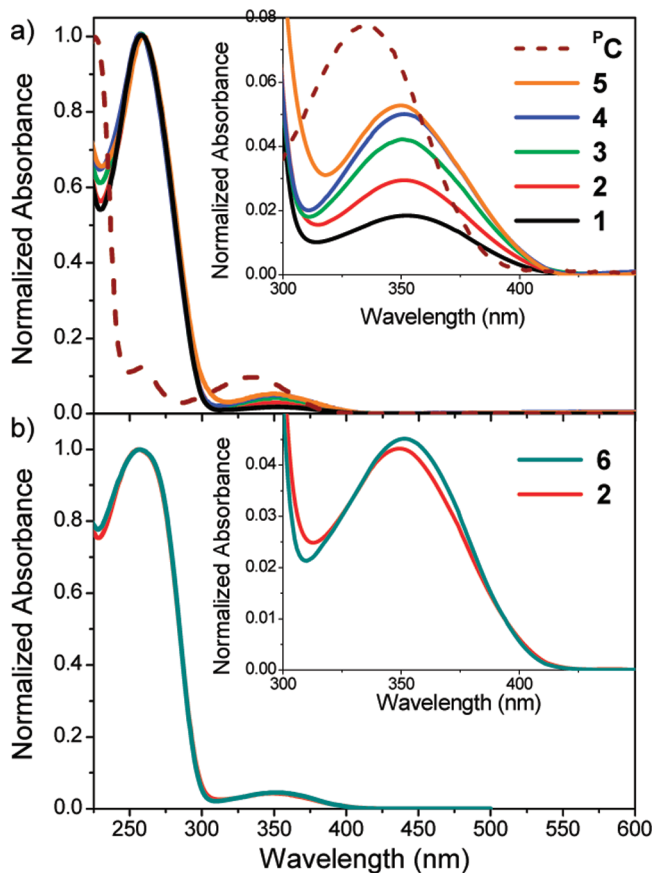


Figure 2. UV–vis spectra of (a) the pyrrolocytosine nucleobase ^PC (14 μ M) and the hairpins 1–5 and (b) 2 and 6 in 10 mM phosphate buffer (pH 7.2) containing 100 mM NaCl. Insets show the longer wavelength region of these spectra. The spectrum of ^PC was normalized at 226 nm, and those of 1–6 were normalized at 260 nm. Concentrations of 1–6 are 17, 8.1, 5.8, 4.2, 3.3, and 8.5 μ M, respectively.

shown in Figure 2b and Figures S3a and S4a. The UV spectrum of ^PC displays a broad long-wavelength band with a maximum at 333 nm with an absorbance of 5900 M^{−1} cm^{−1}²² and a sharper, stronger band at 225 nm. The lowest energy transition of ^PC calculated using the TD3LYP functional is assigned to a weakly allowed π,π^* transition in the monomer, base-paired, and base-stacked structures.²³ This transition is well separated from the next lowest energy transitions. Thus, the long-wavelength band can be assigned to a single transition, simplifying interpretation of the UV and CD spectra. The long wavelength absorption maximum for 1 is red-shifted by 20 nm with respect to that of ^PC (Table 1), plausibly reflecting the influence of base stacking on the energy of the electronic transition. The shorter wavelength bands of ^PC overlap with the absorption bands of the more numerous natural bases in 1 (Figure 2a), making it difficult to evaluate its spectral shift.

The long wavelength absorption maxima for 1–5 display a small continuous blue shift as the length of the ^PC array increases, the magnitude of this shift decreasing as the length of the array increases (Table 1). A similar small blue shift is observed for duplexes possessing 1–3 sequential benzothiazole-modified adenosine base-paired with thymine.¹⁷ However, a small red-shift is observed for duplexes possessing neighboring vs non-neighboring AP chromophores.²⁵ The spectra of 2 and 6 normalized at 260 nm display a blue shift similar to that for 2 vs 1 (Figure 2b) consistent with the assignment of the blue shift for 2 to exciton coupling between neighboring ^PC chromophores. The integrated areas of the long wavelength bands of 2 and 6 are essentially the same, indicating that little hypochromism (<5%) results from a single ^PC–^PC stacking interaction. The UV spectra of 7–9 (Figure S4a) are similar to that of 6, indicating that interstrand as well as intrastrand non-nearest-neighbor interactions are weak. A plot of the long-wavelength absorption maxima vs the number of ^PC chromophores for 1–5 (Figure 3a) is approximately linear for 1–4; however, the value for 5 lies below the fit to the data for 1–4.³² The “missing” 350 nm intensity in the UV spectrum of 5 appears at wavelengths below 320 nm, suggestive of a

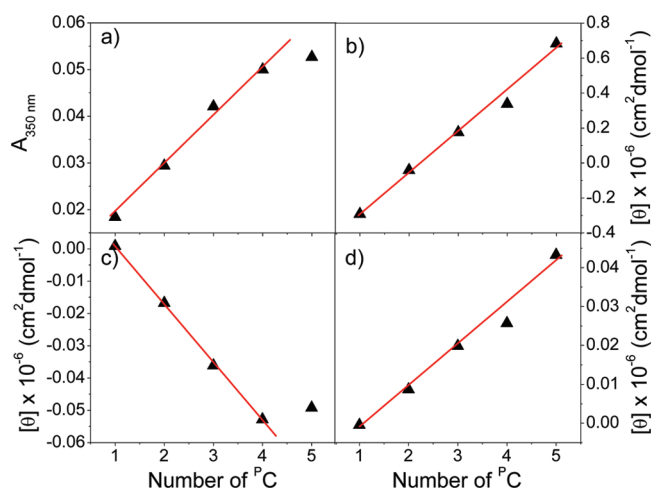


Figure 3. Plots showing the variation in the intensities of UV–Vis and CD spectra of the hairpins 1–5 with increasing number of ^PC chromophores in 10 mM phosphate buffer (pH 7.2) containing 100 mM NaCl. (a) UV–vis spectra at 350 nm; (b–d) CD spectra at 235, 338, and 375 nm, respectively.

nonstandard B-DNA geometry for all or part of the chromophore array.

Circular Dichroism. The CD spectra of solutions of 1–5 and 7–9 having equal 350 nm absorbance are shown in Figure 4 with the long wavelength bands shown in the insets (note the

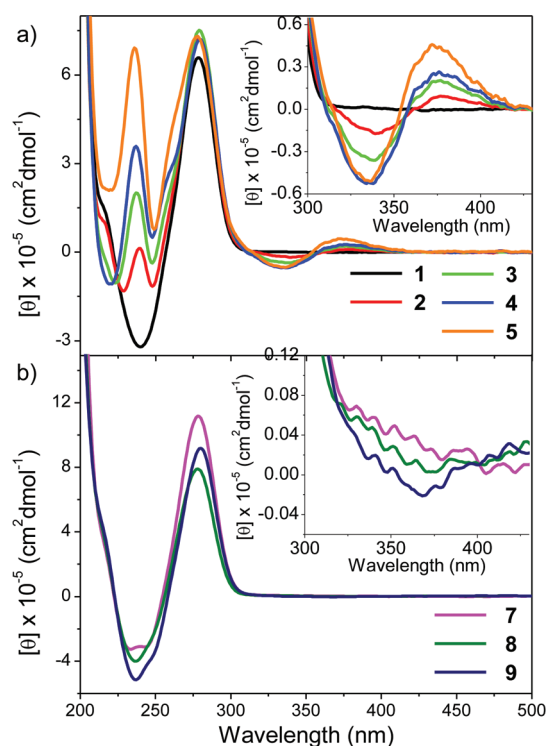


Figure 4. Circular dichroism (CD) spectra of the hairpins (a) 1–5 and (b) 7–9 in 10 mM phosphate buffer (pH 7.2) containing 100 mM NaCl. Insets show the longer wavelength region of these spectra. Concentrations of 1–5 and 7–9 are 17, 8.1, 5.8, 4.2, 3.3, 9.3, 7.7, and 8.3 μM , respectively.

different Y-axes for the insets in Figure 4a,b). The CD spectrum of 1 is similar to that of a hairpin having a C-G rather than a $^{\text{P}}\text{C}$ -G base pair.²⁸ The 200–300 nm region of the CD spectrum of 1 displays a positive band at 280 nm and a negative band at 245 nm (positive Cotton effect) with a node at 260 nm, near the absorption maximum of the duplex. The weak long-wavelength signal for 1 is typical of conjugates having a single achiral aromatic chromophore incorporated into a DNA duplex and is attributed to the induced CD of the chromophore.³³ The CD spectrum of 2 displays strong bands similar to those of 1 and two additional sets of bands. The positive band at 375 nm and negative band at 330 nm are similar to those reported by Johnson et al. for a duplex possessing a $^{\text{P}}\text{C}$ - $^{\text{P}}\text{C}$ step. In addition, we observe a positive band near 235 nm and negative band near 220 nm. These pairs of bands have nodes near the two lowest energy π,π^* transitions of the $^{\text{P}}\text{C}$ chromophores and thus are assigned to exciton coupling between the neighboring $^{\text{P}}\text{Cs}$.¹ The positive and negative bands are of comparable intensity, and thus the spectra are conservative. The greater CD intensity and narrower bands at shorter wavelengths are consistent with the differences in UV band intensity and bandwidth for the short- vs long-wavelength bands of $^{\text{P}}\text{C}$.³⁴

The CD spectra of 7–9 display strong bands in the 200–300 nm spectral region similar to those of 1 but weak bands for wavelengths corresponding to the EC-CD bands of 2. A weak

positive band at 240 nm superimposed on the much stronger negative band is observed for 7 but not for 8 or 9. Very weak nonconservative bands are observed at long wavelengths for 7–9. The absence of strong exciton coupling between $^{\text{P}}\text{C}$ chromophores separated by 1–3 A-T base pairs in 7–9 (Figure 4b) stands in contrast to the observation of EC-CD for stilbenedicarboxamide or perylenediimide chromophores separated by as many as 11 and 13 A-T base pairs, respectively. This difference is due, at least in part, to the much smaller oscillator strength of the lowest energy π,π^* transition $^{\text{P}}\text{C}$ ($\epsilon = 5900 \text{ M}^{-1} \text{ cm}^{-1}$)²² vs stilbene ($35\,000 \text{ M}^{-1} \text{ cm}^{-1}$)⁸ or perylenediimide ($80\,000 \text{ M}^{-1} \text{ cm}^{-1}$).³⁵

The CD spectra of 3–5 display exciton coupled bands at short and long wavelength similar to those of 2 (Figure 4a). The positive bands near 373 and 240 nm and negative bands near 335 nm increase in intensity and display small blue-shifts in the band maximum as the number of $^{\text{P}}\text{C}$ chromophores increases (Figure 3b–d). A similar increase in intensity of EC-CD bands is observed for duplexes possessing 1–3 sequential benzothiazole-modified adenosines base-paired with thymine.¹⁷ Plots of rotational strength vs number of chromophores are approximately linear, with largest deviations observed for $n = 5$, as is the case for the plot of absorbance vs n (Figure 3a). The approximately linear increase in these plots is consistent with domination of the CD spectrum by nearest-neighbor interactions. Deviations from linearity for the longest $^{\text{P}}\text{C}$ tract in 5 can be attributed to deviations from B-DNA geometry as well as minor contributions from non-nearest-neighbor electronic interactions.

The absence of detectable long-range exciton coupling between the electronic transitions of the $^{\text{P}}\text{C}$ chromophores in 2–5 stands in marked contrast to the strong coupling observed for helical arrays of chiral oligo(*p*-phenylenevinylene) (OPV) derivatives.⁶ The absence of strong non-neighboring interactions between the π -stacked bases avoids the large UV spectral shifts observed for these chiral arrays and recently predicted for helical chromophore arrangements such as those in DNA.⁵ The absence of large red-shifts protects cellular DNA from extensive damage by UVA radiation.

CONCLUDING REMARKS

In summary, we have prepared a series of DNA hairpins having 1–5 consecutive $^{\text{P}}\text{C}$ chromophores or two separated chromophores either in the same or opposite strands (Chart 1c) and investigated their spectroscopic properties. The incorporation of the base analogue $^{\text{P}}\text{C}$ into stable DNA hairpins makes it possible for the first time to study the electronic interactions between both nearest-neighbor and non-nearest-neighbor chromophores. Inter- and intrastrand electronic interactions between non-neighboring chromophores are found to be much weaker than interactions of neighboring chromophores. Thus, the UV and CD spectra of hairpins 6 and 7–9 are similar to those of hairpin 1. The observation of exciton-coupled circular dichroism for the first and second π,π^* transitions of $^{\text{P}}\text{C}$ provides evidence for stronger electronic interactions between the stacked chromophores of 2–5. However, the approximately linear correlations of both UV and CD band intensities with the number of chromophores and the very small spectral shifts of the absorption maxima require that nearest-neighbor interactions be much stronger than non-nearest-neighbor interactions including those between $^{\text{P}}\text{C}$ chromophores separated by a single natural base pair. Nearest-neighbor interactions also dominate the lowest energy

CD signals of single strand poly(dA) oligomers.¹¹ However, it is not possible to independently investigate non-neighboring interactions between natural bases in DNA due to their overlapping absorption bands.

■ EXPERIMENTAL SECTION

Pyrrolocytosine nucleobase was purchased from Berry & Associates, Inc., Dexter, MI. Its phosphoramidite was purchased from Glen Research Corporation, Sterling, VA, and incorporated into oligonucleotide conjugates following the standard automated synthetic procedures. DNA conjugates were purified by reverse phase HPLC and characterized by MALDI-TOF mass spectrometry. UV/vis and CD spectra were measured in a 5 mm quartz cuvette at room temperature in Perkin-Elmer Lambda 2 and Jasco 815 spectrometers, respectively.

Molecular dynamics (MD) simulations were carried out on three sequences containing the modified cytosine base. The Amber force field was used to model the standard nucleic acids and TIP3P water.³⁶ Charges were derived for the nonstandard ^PC using the restrained electrostatic potential (RESP) fitting procedure. The derived charges and atom types are given in Table S2, Supporting Information. A periodic system consisting of the DNA sequence, neutralizing sodium ions, and an 8 Å buffer of TIP3P water was constructed. An initial minimization followed by a 2 ns equilibration using the NPT ensemble was performed. The temperature was maintained at 300 K with a Langevin thermostat, and the pressure was maintained at 1 bar using the weak coupling algorithm in Amber 10.³⁷ A real space cutoff of 12 Å was used with long-range electrostatics handled by the particle mesh Ewald summation.

■ ASSOCIATED CONTENT

■ Supporting Information

Chart showing structures of reference hairpins and tables and figures showing *m/z* data, calculated twist angles, and RESP charges for ^PC, UV melting curves of 1–9, and UV and CD of 6–9. This material is available free of charge via the Internet at <http://pubs.acs.org>.

■ AUTHOR INFORMATION

Corresponding Author

*E-mail: fdl@northwestern.edu.

Notes

The authors declare no competing financial interest.

■ ACKNOWLEDGMENTS

Funding for this project was provided by the National Science Foundation (NSF-CRC Grant CHE-0628130).

■ ABBREVIATIONS

^PC, pyrrolocytosine; AP, 2-aminopurine.

■ REFERENCES

- (1) Cantor, C. R.; Schimmel, P. R. *Biophysical Chemistry*; W.H. Freeman: New York, 1980; Vol. 2.
- (2) Cadet, J.; Vigny, P. In *The Photochemistry of Nucleic Acids*; Morrison, H., Ed. Wiley: New York, 1990.
- (3) Taylor, J. S. *Acc. Chem. Res.* **1994**, *27*, 76–82.
- (4) Crespo-Hernandez, C. E.; Cohen, B.; Hare, P. M.; Kohler, B. *Chem. Rev.* **2004**, *104*, 1977–2019.
- (5) Dick, B. *ChemPhysChem* **2011**, *12*, 1578–1587.
- (6) van Dijk, L.; Bobbert, P. A.; Spano, F. C. *J. Phys. Chem. B* **2009**, *114*, 817–825.

- (7) (a) Jonkheijm, P.; van der Schoot, P.; Schenning, A. P. H. J.; Meijer, E. W. *Science* **2006**, *313*, 80–83. (b) Spano, F. C.; Meskers, S. C. J.; Hennebicq, E.; Beljonne, D. *J. Am. Chem. Soc.* **2007**, *129*, 7044–7054.
- (8) Lewis, F. D.; Zhang, L.; Liu, X.; Zuo, X.; Tiede, D. M.; Long, H.; Schatz, G. C. *J. Am. Chem. Soc.* **2005**, *127*, 14445–14453.
- (9) Hariharan, M.; Siegmund, K.; Zheng, Y.; Long, H.; Schatz, G. C.; Lewis, F. D. *J. Phys. Chem. C* **2010**, *114*, 20466–20471.
- (10) (a) Banyasz, A.; Vayá, I.; Chagenet-Barret, P.; Gustavsson, T.; Douki, T.; Markovitsi, D. *J. Am. Chem. Soc.* **2011**, *133*, 5163–5165. (b) Pan, Z.; Hariharan, M.; Arkin, J. D.; Jalilov, A. S.; McCullagh, M.; Schatz, G. C.; Lewis, F. D. *J. Am. Chem. Soc.* **2011**, *133*, 20793–20798.
- (11) Kadhane, U.; Holm, A. I. S.; Hoffmann, S. V.; Nielsen, S. B. *Phys. Rev. E* **2008**, *77*, 021901.
- (12) González, L.; Escudero, D.; Serrano-Andrés, L. *ChemPhysChem* **2012**, *13*, 28–51.
- (13) (a) Sinkeldam, R. W.; Greco, N. J.; Tor, Y. *Chem. Rev.* **2010**, *110*, 2579–2619. (b) Wilson, J. N.; Kool, E. T. *Org. Biomol. Chem.* **2006**, *4*, 4265–4274. (c) Wilhelmsson, L. M. Q. *Rev. Biophys.* **2010**, *43*, 159–183.
- (14) (a) Engman, K. C.; Sandin, P.; Osborne, S.; Brown, T.; Billeter, M.; Lincoln, P.; Nordén, B.; Albinsson, B.; Wilhelmsson, L. M. *Nucleic Acids Res.* **2004**, *32*, 5087–5095. (b) Sandin, P.; Börjesson, K.; Li, H.; Mårtensson, J.; Brown, T.; Wilhelmsson, L. M.; Albinsson, B. *Nucleic Acids Res.* **2008**, *36*, 157–167.
- (15) (a) Genereux, J. C.; Barton, J. K. *Chem. Rev.* **2010**, *110*, 1642–1662. (b) Marti, A. A.; Jockusch, S.; Li, Z.; Ju, J.; Turro, N. J. *Nucleic Acids Res.* **2006**, *34*, e50. (c) Shin, D.; Sinkeldam, R. W.; Tor, Y. *J. Am. Chem. Soc.* **2011**, *133*, 14912–14915.
- (16) (a) Janssen, P. G. A.; Vandenbergh, J.; van Dongen, J. L. J.; Meijer, E. W.; Schenning, A. P. H. J. *J. Am. Chem. Soc.* **2007**, *129*, 6078–6079. (b) Malinovskii, V. L.; Samain, F.; Häner, R. *Angew. Chem., Int. Ed.* **2007**, *46*, 4464–4467.
- (17) Masaki, Y.; Ohkubo, A.; Seio, K.; Sekine, M. *Bioorg. Med. Chem.* **2010**, *18*, 567–572.
- (18) (a) Chen, W.; Schuster, G. B. *J. Am. Chem. Soc.* **2011**, *134*, 840–843. (b) Fendt, L.-A.; Bouamaied, L.; Thöni, S.; Amiot, N.; Stulz, E. J. *Am. Chem. Soc.* **2007**, *129*, 15319–15329. (c) Nakamura, M.; Murakami, Y.; Sasa, K.; Hayashi, H.; Yamana, K. *J. Am. Chem. Soc.* **2008**, *130*, 6904–6905. (d) Nakamura, M.; Ohtoshi, Y.; Yamana, K. *Chem. Commun.* **2005**, 5163–5165. (e) Nakamura, M.; Shimomura, Y.; Ohtoshi, Y.; Sasa, K.; Hayashi, H.; Nakano, H.; Yamana, K. *Org. Biomol. Chem.* **2007**, *5*, 1945–1951. (f) Varghese, R.; Wagenknecht, H.-A. *Chem.—Eur. J.* **2010**, *16*, 9040–9046.
- (19) Asanuma, H.; Shirasuka, K.; Takarada, T.; Kashida, H.; Komiyama, M. *J. Am. Chem. Soc.* **2003**, *125*, 2217–2223.
- (20) (a) Baumstark, D.; Wagenknecht, H.-A. *Chem.—Eur. J.* **2008**, *14*, 6640–6645. (b) Mayer-Enthart, E.; Wagenknecht, H.-A. *Angew. Chem., Int. Ed.* **2006**, *45*, 3372–3375. (c) Wilson, T. M.; Zeidan, T. A.; Hariharan, M.; Lewis, F. D.; Wasielewski, M. R. *Angew. Chem., Int. Ed.* **2010**, *49*, 2385–2388.
- (21) (a) Dallmann, A.; Dehmel, L.; Peters, T.; Mügge, C.; Griesinger, C.; Tuma, J.; Ernstring, N. P. *Angew. Chem., Int. Ed.* **2010**, *49*, 5989–5992. (b) Reha-Krantz, L. J.; Hariharan, C.; Subuddhi, U.; Xia, S.; Zhao, C.; Beckman, J.; Christian, T.; Konigsberg, W. *Biochemistry* **2011**, *50*, 10136–10149. (c) Ward, D. C.; Reich, E.; Stryer, L. *J. Biol. Chem.* **1969**, *244*, 1228–1237.
- (22) Liu, C.; Martin, C. T. *J. Mol. Biol.* **2001**, *308*, 465–475.
- (23) Thompson, K. C.; Miyake, N. *J. Phys. Chem. B* **2005**, *109*, 6012–6019.
- (24) Berry, D. A.; Jung, K.-Y.; Wise, D. S.; Sercel, A. D.; Pearson, W. H.; Mackie, H.; Randolph, J. B.; Somers, R. L. *Tetrahedron Lett.* **2004**, *45*, 2457–2461.
- (25) Rist, M.; Wagenknecht, H.-A.; Fiebig, T. *ChemPhysChem* **2002**, *3*, 704–707.
- (26) Johnson, N. P.; Baase, W. A.; von Hippel, P. H. *Proc. Natl. Acad. Sci. U. S. A.* **2004**, *101*, 3426–3431.
- (27) Johnson, N. P.; Baase, W. A.; von Hippel, P. H. *Proc. Natl. Acad. Sci. U. S. A.* **2005**, *102*, 7169–7173.

(28) Yoshizawa, S.; Kawai, G.; Watanabe, K.; Miura, K.; Hirao, I. *Biochemistry* **1997**, *36*, 4761–4767.

(29) Walker, G. T. *Nucleic Acids Res.* **1988**, *16*, 3091–3099.

(30) Baumstark, D.; Wagenknecht, H.-A. *Angew. Chem., Int. Ed.* **2008**, *47*, 2612–2614.

(31) For structures of duplexes possessing a single AP-C base pair at midstrand in solution and the solid state see refs 21b and 21c.

(32) Hairpin concentrations were calculated in two ways which provide similar results. The values reported in the footnotes to Figure 2 were obtained from the measured 260 nm absorbance and the value obtained from an on-line calculator. These values were in good agreement with those obtained from the measured 350 nm absorbance and the literature value for the nucleobase PC.

(33) Ardhammar, M.; Kurucsev, T.; Nordén, B. In *Circular Dichroism, Principles and Applications*; Berova, N., Nakanishi, K., Woody, R. W., Eds.; Wiley-VCH: New York, 2000; pp 741–768.

(34) Harada, N.; Nakanishi, K. *Circular Dichroic Spectroscopy: Exciton Coupling in Organic Stereochemistry*; University Science Books: Mill Valley, CA, 1983.

(35) Gosztola, D.; Niemczyk, M. P.; Svec, W.; Lukas, A. S.; Wasielewski, M. R. *J. Phys. Chem. A* **2000**, *104*, 6545–6551.

(36) Cheatham, T. E.; Cieplak, P.; Kollman, P. A. *J. Biomol. Struct. Dyn.* **1999**, *16*, 845–862.

(37) Case, T. A. D. D. A.; Cheatham, I., T. E.; Simmerling, C. L.; Wang, J.; Duke, R. E.; Luo, R.; Crowley, R. C. W. M.; Zhang, W.; Merz, K. M.; Wang, B.; Hayik, S.; Roitberg, A.; Seabra, G.; Kolossváry, I. K. F. W.; Paesani, F.; Vanicek, J.; Wu, X.; Brozell, S. R.; Steinbrecher, T.; Gohlke, H.; Yang, C. T. L.; Mongan, J.; Hornak, V.; Cui, G.; Mathews, D. H.; Seetin, M. G.; Sagui, C.; Babin, V.; Kollman, P. A. University of California, San Francisco, 2008.